Hybridization of Cr $3d$ – N $2p$ – Ga $4s$ in the wide band-gap diluted magnetic semiconductor Ga$_{1-x}$Cr$_x$N

J. J. Kim,[1] H. Makino,[2] K. Kobayashi,[3] Y. Takata,[4] T. Yamamoto,[5] T. Hanada,[2] M. W. Cho,[2] E. Ikenaga,[3] M. Yabashi,[3] D. Miwa,[4] Y. Nishino,[4] K. Tamasaku,[4] T. Ishikawa,[4] S. Shin,[4] and T. Yao[1,2]

[1]*Center for Interdisciplinary Research, Tohoku University, Aramaki-Aza-Aoba, Aoba-ku, Sendai 980-8578, Japan*

[2]*Institute for Materials Research, Tohoku University, Sendai 980-8577, Japan*

[3]*JASRI/SPring-8, 1-1-1 Kouto, Mikazuki-cho, Sayo-gun, Hyogo 679-5198, Japan*

[4]*RIKEN/SPring-8, 1-1-1 Kouto, Mikazuki-cho, Sayo-gun, Hyogo 679-5148, Japan*

[5]*Department of Electronic and Photonic Systems Engineering, Kochi University of Technology, 185 Miyanokuchi, Tosayamada-cho, Kamigun, Kochi 782-8502, Japan*

We observed that Cr doping introduces an electronic state in the band gap in Ga$_{1-x}$Cr$_x$N by using hard x-ray photoemission spectroscopy. Based on first-principles calculations, the electronic state is interpreted to be dominantly Ga $4s$ originated states. The chemical effect of Cr up to the second-nearest-neighbor Ga atoms has also been observed in the core-level spectra of Ga $2p_{3/2}$. The present results evidence that the Ga valence electrons are strongly affected by the second-nearest-neighbor Cr atoms through Cr $3d$-Ga $4s$ hybridization.

Hole-mediated ferromagnetism based on the Zener model has produced reliable estimates of Curie temperature (T_c) for diluted magnetic semiconductors (DMS), such as GaMnAs, and predicts that GaMnN will have a T_c above room temperature (RT) if doped with a high hole concentration at about 1×10^{20} cm^{-3} (Refs. 1 and 2). This theory basically assumes that the ferromagnetism occurs through interactions between the local moments of the transition-metal (TM) atoms, which are mediated by the itinerant holes in the material. Okabayashi *et al.* reported some experimental results, which could indicate that the holes introduced by divalent Mn in GaAs occupies an effective-mass Bohr orbit[1–3] and supports the theoretical approximation of hole-mediated ferromagnetism, by using soft x-ray photoemission spectroscopy to classify the GaMnAs as a charge-transfer insulator.[4] They also reported observing overlapping of the Mn $3d$ component with the valence band of GaAs by using resonant photoemission spectroscopy at the photon energies below 70 eV and have asserted that a significant amount of Mn $3d$ character is mixed in the doped holes.[5]

Since doped transition metals introduce deep levels in wide band-gap semiconductors like GaN, and carriers are localized in these states, it may be difficult to apply the hole-mediated ferromagnetism model to wide band-gap GaN-based DMS. The experimentally confirmed Mn$^{3+/2+}$ acceptor level in GaN shows it is very deep in the band gap, Ev +1.8 eV,[6] and thus would be an ineffective p-type dopant under most conditions. Therefore, a different mechanism for magnetism will play a role in GaN-based DMS rather than hole-mediated ferromagnetism. In order to get insight into the mechanism of the magnetism, an electronic structure investigation of GaN-based DMS is necessary.

For the T_c of Mn-doped GaN, a wide range of values from 10 to 940 K,[7–11] has been reported from measurements of magnetic properties. Meanwhile, it is argued that the observed ferromagnetism in Mn-doped GaN arises from ferromagnetic Ga-Mn or Mn-N clusters.[12–14] Therefore, the mag-

netism of Mn-doped GaN is still controversial. On the other hand, recently, the very stable RT ferromagnetism of Cr-doped GaN has been predicted by first principles calculation,[15] and confirmed experimentally.[16–18]

In this communication, we report on the electronic structure of Cr-doped GaN observed by hard x-ray photoemission spectroscopy at an excitation energy of 5.95 keV to understand the origin of the ferromagnetism. Soft x-ray photoemission spectroscopy is very surface sensitive due to the short mean-free paths of electrons at measurable kinetic energies. There is no method for making an ideal surface after exposure to atmosphere even once. This problem is more serious for the case of epitaxial thin films because surface cleaning procedures are not well established. The photoemission spectra (PES's) of Ga$_{1-x}$Cr$_x$N in this research are actually bulk sensitive, and also almost free from distortion due to inelastic scattering at high energies.[19–21] Thus we are able to precisely analyze the difference of the spectra between doped and undoped GaN.

Epitaxial films of Ga$_{1-x}$Cr$_x$N with a thickness of 300 nm were grown by NH$_3$-assisted molecular beam epitaxy (MBE) on 400-nm-thick ZnO templates. The films have a wurtzite structure with Cr substituting at the Ga sites in GaN without any other secondary phases up to $x=0.101$, and show ferromagnetic behavior above RT. The nominal concentration of Cr was measured by electron probe microanalysis. Details about the MBE epitaxial growth process and Ga$_{1-x}$Cr$_x$N magnetic properties are already published elsewhere.[18] The PES's of the Ga$_{1-x}$Cr$_x$N were measured at undulator beam line, BL29XU (Refs. 22 and 23) and BL47XU, of SPring-8. Hard x rays of 5.95 keV with an energy spread of 75 meV was used. The vacuum of the analyzer chamber was $\sim 10^{-5}$ Pa. The large escape depth at high energy (above 5 nm at 5.95 keV) allows determination of bulk electronic states with high precision owing to negligibly small contribution from the surface,[19] therefore, no surface cleaning was done. Photoelectrons were collected by a Gammadata Sci-
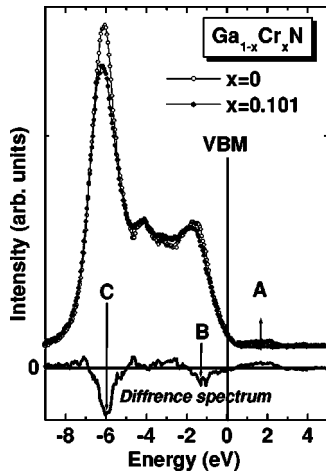
FIG. 1. Energy distribution curves (EDC's) for undoped GaN (open circles) and $Ga_{0.899}Cr_{0.101}N$ (filled circles) at $h\nu=5.95$ keV. These EDC's are obtained by subtracting the trivial background from the experimental spectra. The solid line at the bottom panel shows the difference spectrum.

enta SES2002 electron analyzer system, which is modified to accommodate higher photoelectron kinetic energies up to 6 keV. Energy resolution was estimated to be 310 meV at RT by the Fermi energy (E_F) of Au plates.

In all of the PES's (N 1s, Ga 2$p_{3/2}$, and valence-band spectra), there was a shift of the entire energy to the low binding-energy (BE) region for the $Ga_{0.937}Cr_{0.063}N$ and the $Ga_{0.899}Cr_{0.101}N$, compared to undoped GaN, by 1.1 and 1.2 eV, respectively. Since the as-grown undoped GaN is an n-type semiconductor, the E_F is very near the conduction-band minimum. The shifts of the entire energy that indicate the formation of a localized Cr 3d state in the band gap and the E_F are pinned at the top of the electron filled Cr 3d state. To compare the PES's of $Ga_{1-x}Cr_xN$ with that of undoped GaN, the origins of the binding energy are set to the valence-band maximum (VBM). For quantitative analysis, the N 1s core level PES's were normalized to the area of each spectrum, and the Ga 2$p_{3/2}$ core level and the valence-band PES's were scaled by the same factor as the corresponding N 1s spectra. This scaling is valid because we confirmed that Cr does not occupy an interstitial or N site, but the Ga site by x-ray diffraction and angular dependent N 1s x-ray absorption results.[18,24]

Open circles, filled circles, and the solid line in Fig. 1 show the normalized energy distribution curves (EDC's) of undoped GaN, that of $Ga_{0.899}Cr_{0.101}N$, and the difference spectrum between them, respectively. The Cr doping does introduce, clearly, new electronic levels in the band gap (**A**) and causes some change in the valence-band structure (**B** and **C**).

To elucidate the origin of the new electronic states, we have calculated the electronic band structure for Cr-doped GaN based on the density-functional theory (DFT)[25] using the generalized gradient approximation (GGA).[26] The cell is optimized with the Vienna *ab initio* simulation package (VASP)[27] based on the projector-augmented-wave approach[28] with the following parameters: k spacing of
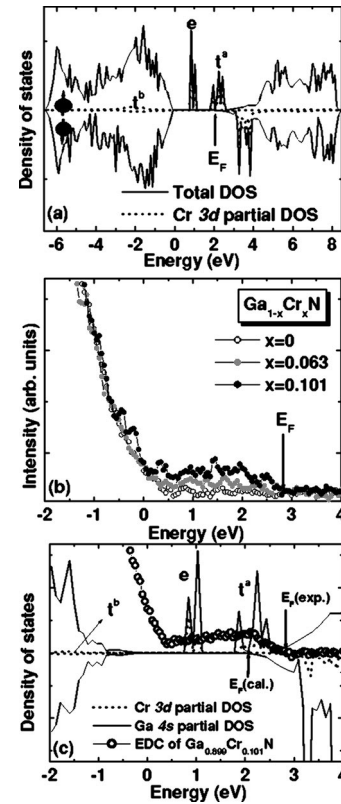

FIG. 2. (a) Calculated total DOS and Cr 3d partial DOS based on the DFT with GGA. (b) EDC's near the VBM of the undoped GaN (open circles) and the $Ga_{1-x}Cr_xN$ [$x=0.063$ (solid gray circles), 0.101 (solid black circles)]. The intensity of the new energy state in the band gap depends on the Cr concentration. (c) The comparison between the EDC (open circles) of the $Ga_{0.899}Cr_{0.101}N$ and the quantitatively scaled partial DOS's both of Cr 3d (dotted line) and Ga 4s (solid line) in the $Ga_{15}Cr_1N_{16}$ supercell.

0.3 Å, self-consistent-field (SCF) convergence of 1.0×10^{-5} eV, gradient convergence of 0.03 eV/Å, and Gaussian smearing. We calculated the crystal structures of GaN with periodic boundary conditions by generating a supercell that contained the objects of interest. For GaN doped with Cr, we replace one of the 16 sites of Ga atoms by a Cr site in the supercell model.

The solid and the dotted lines in Fig. 2(a) show the total density of states (DOS) and Cr 3d partial DOS. There are two sharp up-spin bands in the band gap. By considering the localized model, the origin of these bands can be explained as follows. Since the Cr atoms in Ga sites are tetrahedrally bonded with four nitrogens, $3d\epsilon$ (dxy, dyz, and dzx orbital) and $3d\gamma$ (dx^2-y^2 and dz^2 orbital) states are separated into nonbonding (**e**), bonding ($\mathbf{t}^b$), and antibonding states ($\mathbf{t}^a$) in the tetrahedral crystal field. The two sharp up-spin bands correspond to the **e** and $\mathbf{t}^a$. The $\mathbf{t}^b$ is merged in the valence band and the down-spin band overlaps the conduction band. Because of E_F positioned at $\mathbf{t}^a$, the up- and down-spin states are separated, thus the material is spin polarized. This calculated result is similar to the DOS calculated by the Korringa-Kohn-Rostoker method combined with the coherent potential approximation.[15] Figure 2(b) shows the EDC's of the $Ga_{1-x}Cr_xN$ ($x=0$, 0.063, and 0.101) near the VBM. Intensi-

ties of the in-gap states proportionally increase with increasing the Cr concentration. Therefore, the in-gap states are closely related to the Cr 3d orbitals.

Based on first-principles calculations, the Cr 3d mainly contributes to the in-gap states. However, the atomic subshell photoionization cross section of Cr 3d (4×10^{-7} Mb for $Ga_{0.899}Cr_{0.101}N$) is very small compared to Ga 4s (5.4×10^{-5} Mb for $Ga_{0.899}Cr_{0.101}N$) at the high excitation energy.[29] In our calculation, the second-nearest-neighbor Ga 4s also contributes to the in-gap states by the hybridization with Cr 3d. Therefore, the question arises which is the main contribution to the observed in-gap states.

We have done two different estimations to solve the problem. First, we compared the Ga 4s and Cr 3d contributions to the in-gap state estimated from our DOS calculation. The solid and the dotted lines in Fig. 2(c) are the Ga 4s and the Cr 3d contributions, respectively. These are obtained from the partial DOS's multiplied by the atomic subshell photoionization cross sections at 6 keV.[29] In case of the Ga 4s contribution, it is also multiplied by 12, considering the 12 coordinated Ga around the Cr atom. The ratio of Ga 4s to Cr 3d contributions to the area of the in-gap state is then estimated to be 3.7. In the second estimation, we calculated the ratio of the area of the observed in-gap state to that of the valence band in the region of 0 to -8 eV, where Ga 4s contribution is dominant, to be 0.021 for $x=0.1$. This ratio is to be compared with the ratio of the Ga 4s partial density of the in-gap state to that of the matrix valence band. Our calculation for $x=0.07$ gives a value of 0.015 for this ratio. After scaling by the Cr concentration, both the experimental and calculated ratios almost coincide at around the value of 0.02 for $x=0.1$. The above two different estimations assure that the new electronic state in the band gap is dominantly of Ga 4s nature.

Cr doping also causes changes in the valence band (**B** and **C** in Fig. 1). Since Cr atoms are positioned at the Ga sites, as described above, the Ga 4s contribution in the Cr-doped GaN decreases compare to undoped GaN. The negative values of the **B** and **C** peaks in the difference spectrum are considered to be primarily due to the decrease of Ga content in the matrix. However, if the difference spectrum is only related to the decrease of Ga content, the shape must resemble the Ga 4s partial DOS of undoped GaN. The energy region from -2 to -5 eV in the difference spectrum is not similar to the Ga 4s partial DOS. This dissimilarity implies that the t^b state, which is distributed in the same energy region as that of the difference spectrum, as shown in Fig. 1, is also responsible for the valence-band change.

We have also investigated the core-level PES's of the N 1s and Ga 2$p_{3/2}$. Open circles, solid gray circles, and solid black circles in Fig. 3(a) show N 1s core-level spectra of undoped GaN, $Ga_{0.937}Cr_{0.063}N$, and $Ga_{0.899}Cr_{0.101}N$, respectively. Gray and black solid lines are the difference spectra between the undoped GaN and $Ga_{1-x}Cr_xN$ ($x=0.063$ and 0.101). The main peak (394.5 eV) decreases and the tail in the low BE region (393.8 eV) increases with Cr doping. The rate of the decrease and the increase is proportional to the Cr concentration. Namely, Cr doping causes a decrease of the N 1s in the matrix and introduces a new chemically shifted component at the low BE region. Because the electronega-
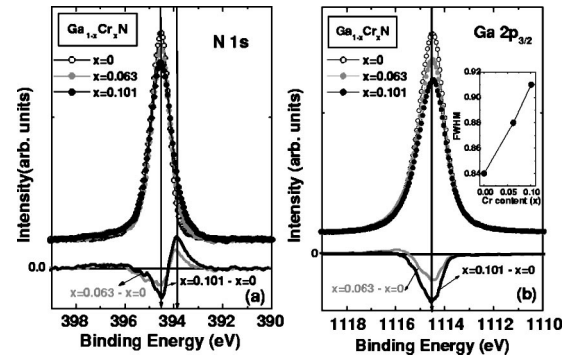

FIG. 3. The core-level PES's of (a) N 1s and (b) Ga 2$p_{3/2}$ of the undoped GaN (open circles) and the $Ga_{1-x}Cr_xN$ [$x=0.063$ (solid gray circles), 0.101 (solid black circles)]. The right inset in (b) shows the FWHM variation of the Ga 2$p_{3/2}$ spectra with Cr concentration. The more Cr doped, the broader the FWHM of Ga 2$p_{3/2}$ spectra.

tivities (EN) of the Ga, Cr, and N atoms are 1.81, 1.56, and 3.07, respectively,[30] the EN difference of the Cr-N bond is larger than that of Ga-N bond. Therefore, the N atoms bonded with Cr are more shielded by electrons compared to the N atom bonded with Ga atoms. Accordingly, Cr doping causes a chemical shift of the N 1s to the low binding-energy side. Figure 3(b) shows Ga 2$p_{3/2}$ core-level spectra of undoped GaN (open circles), $Ga_{0.937}Cr_{0.063}N$ (solid gray circles), and $Ga_{0.899}Cr_{0.101}N$ (solid black circles). Intensity of the peak decreases with Cr doping. Decrease of the intensity is almost linearly proportional to the increase of Cr content. The line shape in difference spectra is evidently asymmetric, suggesting the existence of an unresolved chemical shifted component at the low BE side. This is reasonably expected from the EN differences between Ga-Cr and N-Cr. Linear increase of the full width at half maximum (FWHM) with increasing Cr content [inset in Fig. 3(b)] is taken as further corroboration of the existence of increasing chemical shift component, supporting Ga-Cr hybridization discussed above.

According to the calculated DOS, the Ga 4s is also spin polarized the same as the Cr 3d. By comparing between the mainly Ga 4s originated EDC and the calculated Ga 4s partial DOS, the new electronic states in the band gap corresponds to the **e** and t^a in the band gap. In the experimental result, the E_F position does not agree with the calculation and the electronic states are not separated into the two bands as the calculation shows. The as-grown undoped GaN has unintentionally doped electrons as 8×10^{19} cm^{-3} in the conduction band. The Cr doping results in high resistivity as well as a shift of E_F position to the higher-energy side than the calculated E_F. These are interpreted to be due to almost full compensation of the residual electrons by Cr doping.[31] The ionization impurity concentration then reaches near 1×10^{20} cm^{-3}. This value is considered to be large enough to cause the broadening of the in-gap states due to the spatial fluctuation of the ionized impurity potential. The above results are consistent with the present calculation, that is, the Cr 3d orbital is not only hybridized with the nearest N but also the second-nearest-neighbor Ga atom by Cr-N chemical

bond formation. In 6% Cr doping, the Cr-N-Ga-N-Cr network makes a large island by percolation in the crystal. This island possibly plays an important role in the ferromagnetism of $Ga_{1-x}Cr_xN$.

In conclusion, we have investigated the electronic structure of $Ga_{1-x}Cr_xN$ using bulk sensitive hard x-ray photoemission spectroscopy excited by synchrotron radiation. We have observed the electronic states in the GaN band-gap region induced by Cr doping in GaN host. This is the Ga 4s contribution raised by the hybridization with Cr 3d. In the core-level study, we also observed that the Cr doping influences the second-neighbor Ga via the formation of Cr-N bonds. The correspondence between experimental in-gap hybridized state and the up-spin band in the band gap of the theoretical spin-polarized Ga 4s states leads us a hypothesis that ferromagnetic interaction between distinct Cr atoms is mediated by the Cr 3d–N 2p–Ga 4s hybridization. This may play a significant role in the spin-polarized state and the previously observed ferromagnetism in $Ga_{1-x}Cr_xN$ although more studies, like magnetic circular dichroism studies in the case of the GaMnAs (Ref. 32) or the spin-polarized photoemission spectroscopy, are needed.

[1] T. Dietl, H. Ohno, F. Matsukura, J. Cibert, and D. Ferrand, Science **287**, 1019 (2000).

[2] T. Dietl, H. Ohno, and F. Matsukura, Phys. Rev. B **63**, 195205 (2002).

[3] A. K. Bhattacharjee and C. B. á la Guillaume, Solid State Commun. **113**, 17 (2000).

[4] J. Okabayashi, A. Kimura, O. Rader, T. Mizokawa, A. Fujimori, T. Hayashi, and M. Tanaka, Phys. Rev. B **58**, R4211 (1998).

[5] J. Okabayashi, A. Kimura, T. Mizokawa, A. Fujimori, T. Hayashi, and M. Tanaka, Phys. Rev. B **59**, R2486 (1999).

[6] T. Graf, M. Giukic, M. S. Brandt, M. Stutzmann, and O. Ambacher, Appl. Phys. Lett. **81**, 5159 (2002).

[7] M. E. Overberg, C. R. Abernathy, S. J. Pearton, and N. A. Theodoropoulou, Appl. Phys. Lett. **79**, 1312 (2001).

[8] G. T. Thaler, M. E. Overberg, B. Gila, R. Frazier, C. R. Abernathy, and S. J. Pearton, Appl. Phys. Lett. **80**, 3964 (2002).

[9] N. Theodoropoulou, A. F. Hebard, M. E. Overg, C. R. Abernathy, and S. J. Pearton, Appl. Phys. Lett. **78**, 3475 (2001).

[10] M. L. Reed, N. A. El-Masry, H. H. Stadelmaier, M. K. Ritums, and M. J. Reed, Appl. Phys. Lett. **79**, 3473 (2001).

[11] S. Sonoda, S. Shimizu, T. Sasaki, Y. Yamamoto, and H. Hori, J. Cryst. Growth **237-239**, 1358 (2002).

[12] Y. Shon, Y. H. Kwon, D. Y. Kim, X. Fan, D. Fu, and T. W. Kang, Jpn. J. Appl. Phys., Part 1 **40**, 5304 (2001).

[13] S. Dhar, O. Brandt, A. Trampert, L. Däweritz, K. J. Friedland, K. H. Ploog, J. Keller, B. Beschoten, and G. Güntherodt, Appl. Phys. Lett. **82**, 2077 (2003).

[14] M. Zajac, J. Gosk, E. Grzanka, M. Kamińska, A. Twardowski, B. Strojek, T. Szyszko, and S. Podsiadlo, J. Appl. Phys. **93**, 4715 (2003).

[15] K. Sato and H. KatayamaYoshida, Jpn. J. Appl. Phys., Part 2 **40**, L485 (2001).

[16] S. E. Park, H. J. Lee, Y. C. Cho, S. Y. Jeong, C. R. Cho, and S. L. Cho, Appl. Phys. Lett. **80**, 4187 (2002).

[17] M. Hashimoto, Y. K. Zhou, M. Kanamura, and H. Asahi, Solid State Commun. **122**, 37 (2002).

[18] J. J. Kim, M. Makino, P. P. Chen, T. Suzuki, D. C. Oh, H. J. Ko, J. H. Chang, T. Hanada, and T. Yao, Phys. Status Solidi C **0**, 2869 (2003).

[19] Y. Takata *et al.*, Appl. Phys. Lett. **84**, 4310 (2004).

[20] K. Kobayashi *et al.*, Jpn. J. Appl. Phys., Part 2 **43**, L1029 (2004).

[21] K. Kobayashi *et al.*, Appl. Phys. Lett. **83**, 1005 (2003).

[22] H. Kitamura, J. Synchrotron Radiat. **7**, 121 (2000).

[23] K. Tamasaku, Y. Takata, M. Yabashi, H. Yamazaki, N. Kawamura, M. Suzuki, and T. Ishikawa, Nucl. Instrum. Methods Phys. Res. A **467-468**, 686 (2001).

[24] T. Takeuchi *et al.* (unpublished).

[25] W. Kohn and L. J. Sham, Phys. Rev. **140**, A1133 (1965).

[26] J. P. Perdew, *Electronic Structures of Solids 91*, edited by P. Ziesche and H. Eschrig (Akademie Verlag, Berlin, 1991).

[27] G. Kresse and J. Furthmuller, Phys. Rev. B **54**, 11 169 (1996).

[28] G. Kresse and D. Jöbert, Phys. Rev. B **59**, 1758 (1999).

[29] J. J. Yeh and I. Lindau, At. Data Nucl. Data Tables **32**, 1 (1985).

[30] A. L. Allred and E. G. Rochow, J. Inorg. Nucl. Chem. **5**, 264 (1958).

[31] H. X. Liu, S. Y. Wu, R. Singh, L. Gu, D. J. Smith, N. R. Dilley, L. Montes, M. B. Simmonds, and N. Newman (unpublished).

[32] D. J. Keavney, D. Wu, W. Freeland, E. Johnston-Halperin, D. D. Awschalom, and J. Shi, Phys. Rev. Lett. **91**, 187203 (2003).